J. Condensed Matter Nucl. Sci. 39 (2025) 379–406

Research Article

A Phenomenological Model, Quantum Mechanics and Complexity in the Cold Fusion Phenomenon – A Review

Hideo Kozima

Cold Fusion Research Laboratory, 597-16 Yatsu, Aoi, Shizuoka 421-1202, Japan

Abstract

We have investigated the basis of the TNCF model, a phenomenological model proposed in 1994, using ideas and calculations we gave after the proposal of the model. We have pondered especially a mechanism of deexcitation of an unstable nucleus in transition-metal hydrides/deuterides by interaction with neutrons in neutron bands dissipating energy into lattice oscillation. The mechanism of dissipation of unstable nuclei in transition-metal hydrides seems overwhelmingly more effective than the mechanism of deexcitation by photon emission. The effectiveness seems enormous when there are a lot of neutrons in the neutron bands formed by the super-nuclear interaction between neutrons in lattice nuclei mediated by the strong neutron-proton/deuteron interaction, realized by the non-localized wavefunction of occluded proton/deuteron. The conditions for the formation of neutron bands where the wavefunctions of the occluded proton/deuterons overlap with that of neutrons in lattice nuclei collate closely with the peculiarity of physics and chemistry, such as the super-diffusivity of hydrogen and hydrogen electrode reaction, in transition-metal hydrides.
 ISSN 2227-3123

Keywords: Phenomenology, cold fusion phenomenon, complexity, deexitation, neutron band, neutron Bloch wave, transition-metal hydrides, biotransmutation.

1. Introduction

Two papers published in 1989, one by Fleischmann et al. [1] and another by Jones et al. [2] opened the gate to the solid state-nuclear physics. A paper by H. Kozima published in 1994 [3] marked the beginning of phenomenological approach to the research of the cold fusion phenomenon (CFP) in this solid state-nuclear physics. After about 35 years from the beginning of the research of the science of the CFP, we have time to recollect the structure of our research in this science as it was formed.

First, we give a brief history of the science of the cold fusion phenomenon (CFP) [4], [5], [6], [7] observed in the CF materials composed of main atoms (transition metals, carbon (graphite), biological molecules) and hydrogen isotopes (protons, deuterons).

First of all, we would like to define the cold fusion phenomenon (CFP), the title of our research field. The Cold Fusion Phenomenon (CFP) stands for;

 ISSN 2227-3123

"*Nuclear reactions and accompanying events occurring in open (with external particle and energy supply), non-equilibrium system composed of solids with high densities of hydrogen isotopes (H and/or D) in ambient radiation*" belonging to Solid State-Nuclear Physics (SSNP).

As explained in a recent paper [8], the TNCF model, a phenomenological model based on the experimental facts with an adjustable parameter n_n, the density of trapped neutrons in the CF material, had been so successful that can explain consistently a majority of wonderful events observed in the CFP [4], [5], [6], [7]. We introduced the essence of the model in Section 2. The premises of the TNCF model are overviewed in Appendix A2 based on the description in our book [4].

In response to the surprise of people who met the successful explanation of CFP by the TNCF mode in our book published in 1998 [6 (Sections 10.3 and 10.4)], we cited a few sentences by physicists in the 1910's bewildered with the Bohr's model of atoms in the period of evolution of physics presented in Appendix A1.

We have tried to justify quantum mechanically the premises used in the TNCF model for CFP as shown in our books and papers (e.g., [5], [9], [10], [11], [12]). One of the key concepts in this effort is the neutron bands formed in the CF material by the interaction of neutrons in lattice nuclei and occluded protons/deuterons [5 (Sec. 3.7), 9 (Sec. 3)]. In the process of the quantum mechanical justification of the premises to explain the CFP occurring in CF materials, we noticed existence of the self-organization of optimum conditions in samples shown by the non-linear dynamics as complexity [11]. Furthermore, there are several physical and chemical phenomena consistently explicable using the idea developed in the quantum mechanical effort to explain the premises assumed in the TNCF model [13]. These phases of CFP are discussed in Section 3.

In section 3, we gave an outlook on the existence of the trapped neutrons and an explanation of several premises in relation to the properties of the trapped neutrons using the idea of neutron bands [5], [9], [11]. In the formation of the neutron bands, the key concepts are: (1) the overlapping of the wavefunctions of occluded protons/deuterons and those of neutrons in the adjacent lattice nuclei and (2) the super-nuclear interactions between neutrons in different lattice nuclei mediated by protons/deuterons occluded in the CF material [5 (Section 3.7), 9 (Section 3), 11].

Another key concept of the TNCF model is the amazing role of the neutron Bloch wave stabilizing unstable nucleus in the CF material: (1) the dissipation of excitation energy of nuclei to the lattice as excess heat not by gamma emission and (2) acceleration of the decay processes of radioactive nuclei, both by the interaction with the neutron Bloch wave in the neutron bands. We recollect basic research into the interaction of nuclei with electromagnetic radiation by Blatt and Weisskopf [14] in Appendix A4, and give an idea of how to explain the mechanism of the dissipation. This is one of the premises taken up in Section 3, which was left as a problem as pointed up in our paper [8]. An attempt to investigate the role of the neutron Bloch wave in the stabilization of unstable nucleus is taken up in Appendix A5 with a brief review of experimental data and a blueprint for the solution.

2. TNCF Model (A Phenomenological Model) for the Cold Fusion Phenomenon

A phenomenological approach to the cold fusion phenomenon (CFP) was tried in 1994 [3] using the trapped neutron catalyzed fusion (TNCF) model. We were able to give a consistent explanation for important experimental data sets obtained in this field [8]. The premises assumed in the model have been investigated and some of them have been given a quantum-mechanical basis. We examine the phenomenological model and describe the structure of the TNCF model in this section.

2.1. Impacts of Phenomenological Models

There have been several models that played key roles in the history of science. We give the structure and impact of one of the most famous models, Bohr's model of the atom, in Appendix A1.

The success of Bohr's model giving a cornerstone for the birth of quantum mechanics tells us of the importance of diverse approaches to a problem based on principles different from, and alien to, those prevailing in science at the time.

2.2. Premises of the TNCF Model

In our phenomenological approach using the TNCF model [3], [4], [5], we have used several premises not necessarily explained theoretically by the existing science even if there are incomplete efforts to understand them [5], [9], [11]. Two important problems related to the premises of the model should be investigated seriously [8].

We have enumerated the premises assumed in the TNCF model in Appendix A2 to refer later in the course to explain some of them quantum-mechanically in Sections 3.3 and 3.4.

In the following Subsection 2.3, we give brief explanations of several examples observed in four genres of CFP, (1) metal hydrides/deuterides, (2) hydrogen graphite, (3) XLPE (cross-linked polyethylene), and (4) biological systems.

2.3. Examples of CFP in Metal Hydrides/Deuterides, Hydrogen Graphite, XLPE (Cross-Linked Polyethylene) and Biological Systems explained by TNCF Model

Concerted investigation of the cold fusion phenomenon (CFP) started after the 1989 announcement of the discovery of nuclear reactions in the palladium deuteride $\mathrm{PdD_x}$ [1]. The authors of the original paper unequivocally asserted that the mechanism of the nuclear reactions of the CFP in the *d–d* fusion reactions [15] even if there was general opposition to this idea based on the quantum mechanical basis to achieving the reaction by overwhelming the Coulomb barrier between charge nuclei in solids without any acceleration mechanism. The investigation of the CFP has developed revealing existence of nuclear reactions in various materials where coexist hydrogen isotopes (H and/or D) and regularly arranged nuclei (C, Ti, Ni, Pd etc.) having outermost neutrons with extended wavefunctions [16 (Sec. 2.7)]. We summarize these features of the CFP in this subsection.

2.3.1. *Metal Hydrides/Deuterides*

(a) $\mathbf{PdD_x}$ ($\mathbf{x \lesssim 1}$) The experimental data sets published by McKubre et al. in 1993 and 1994 [17], [18], [19] in the same $\mathrm{PdD_x}$ system as that used by Fleischmann et al. with a more sophisticated calorimeter are the most extensive one ever obtained in this system. We have investigated the elaborate result by McKubre et al. and elucidated its indispensable value for the science of the CFP [20 (Sec. 3.4)]. We just note this fact here.

(b) $\mathbf{NiH_x}$ ($\mathbf{x \lesssim 1}$) In the long history of the CFP research, there are many important and interesting works in the transition-metal protium system [4 (Sec. 7), 5 (Sec. 2.2.1)]. The first report of the CFP in a protium system is, as far as I know, the one by R.L. Mills and S.P. Kneizys which was appeared in 1991 [21]. The second was by R.T. Bush also published in 1992 [22]. These papers reported the excess heat generation in protium systems.

The first direct evidence of the nuclear reactions in protium systems was measured by R.T. Bush and R.D. Eagleton in 1993 [23], [24].

We have analyzed their data using our TNCF model applicable to deuterium and also protium systems [4 (Sec.9.1b)] and have given a semi-quantitative explanation of their observation of transmuted nuclei [23].

2.3.2. *Hydrogen Graphite*

In the carbon arc system with graphite electrodes in water, there are found many kinds of elements in addition to the most abundant, iron (Fe); Si, S, Cl, K, Ca, Ti, Cr, Mn, Co, Ni, Cu, Zn, and possibly heavier elements

In the experiments performed by T. Hanawa [25], he found various new elements and changes of quantities of elements in the product of carbon arc with graphite electrodes in light water using energy dispersive X-ray spectrometry, method of X-ray fluorescence (XRF) and particle induced X-ray emission.

The experimental results obtained in carbon arc are very difficult to understand, similar to the data obtained in XLPE and biological systems, which are introduced following subsections. However, we may be able to treat the data in these carbon-hydrogen systems using our TNCF model as explained in this section.

We may have a superlattice made of a carbon sublattice of graphite and a hydrogen sublattice occluded between carbon layers in the graphite electrodes covered by a CO_2 layer [26, 27(Sec. 3.7.1)]. If the hydrogen graphite HC_x forms such a superlattice considered in the paper cited above, this forms CF-matter which participates in the CFP by the mechanism proposed in our book [5 (Sec. 3.7)]. Thus, the product elements observed in the system of carbon arc in water are explained by our TNCF model as a result of the nuclear transmutation catalyzed by the trapped neutrons.

2.3.3. *XLPE*

The excellent experimental data on nuclear transmutation in cross-linked polyethylene had been obtained by Kumazawa et al. for more than 10 years starting in 2005 [28], [29], [30].

The experimental data obtained by Kumazawa et al. [28], [29] have successfully been analyzed by the TNCF model as explained by our paper [31]. The superlattice of C and H in the XLPE works to generate neutron bands according to the mechanism figured out in the TNCF model and the neutrons in the bands thus formed induce nuclear reactions and produce new elements observed by Kumazawa et al. Recent data of gamma emission from XLPE [30] is analyzed using the TNCF model successfully and the result is presented in a paper [31].

2.3.4. *Biological Systems*

The biotransmutation, i.e., the nuclear transmutations in biological systems, has been investigated for more than 200 years since L.N. Vauquelin observed a large quantity of lime (CaO) in the daily excretions of chickens in 1799 [4 (Sec. 10.1)].

The recent experimental data sets on the nuclear transmutations in biological systems have mainly been obtained over the last 20 years by V.I. Vysotskii and his collaborators [32], [33], [34], [35]. There are data sets showing (1) production of $^{57}{}_{26}$Fe from $^{55}{}_{25}$Mn [32], [35] and also (2) acceleration of the decay of radioactive nuclei $^{157}{}_{55}$Cs, $^{140}{}_{56}$Ba and $^{140}{}_{57}$La in several microbial cultures [34], [35].

The complex structures of biological cells, a part of which are shown in Figs. 3.7.4 and 3.7.5 of our paper [27], have regular arrays of molecules made of carbon and hydrogen, similar to the array found in XLPE in the rather simple form discussed in the previous section. The superlattices found in these biological systems might be able to generate neutron bands as in the case of XLPE where we can assume the CF matter to induce the CFP as observed by Vysotskii et al. Details of the treatment are given in another paper [36].

3. Nuclear Interaction between Neutrons in Lattice Nuclei and Occluded Protons/Deuterons in Interstices

There are many experimental facts about the electrical and chemical properties of the transition-metal hydrides piled up in more than a hundred years in solid state physics [7 (Sec. 3.6)]. In the experimental data, there are several riddles that seemingly have a close relation with the mechanism of the CFP awaiting a consistent explanation but not given appropriate explanations yet [13].

In this section, we summarize several facts about wavefunctions of occluded protons/deuterons in the transition-metal hydrides/deuterides and wavefunctions of neutrons in a nucleus having a close relationship to CFP.

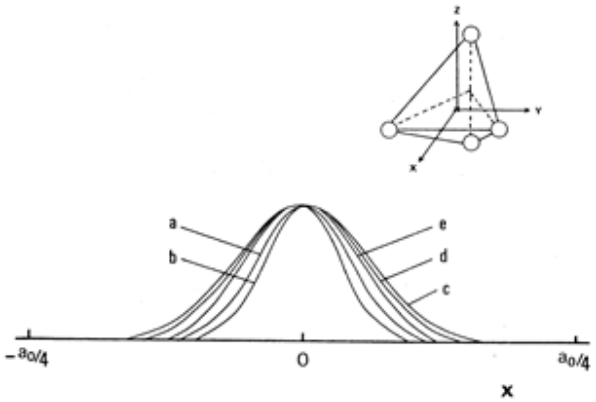

Figure 1. Density profiles of H and D on T-sites in *bcc* metals (Nb, V, Ta) in the x-direction shown in the inset. Profiles calculated for a) an H-atom and b) a D-atom in Nb. Profiles observed by Reidinger et al. for c) $VD_{0.79}$ at 70 °C, d) $NbH_{0.82}$ at 119 °C and $NbD_{0.73}$ at 140 °C and e) $TaH_{0.20}$ at 150 °C. (Fig. 5 of H. Sugimoto and Y. Fukai, *J. Phys. Soc. Japan* **51** (8), pp. 2554–2561 (1982)).

3.1. Wavefunctions of an Occluded Proton/Deuteron in fcc Transition Metals [10, 37]

We give essential characteristics of the wavefunctions of occluded protons/deuterons in transition-metal hydrides/deuterides in this Section, leaving more detailed treatments in Appendix A3, Non-localized Wavefunctions of Hydrogen in *fcc* Transition Metals.

The difference of the wavefunctions of occluded protons/deuterons in transition-metal hydrides/deuterides with bcc and fcc structure should be emphasized first of all, as described in the following quotes:

"The nature of the wavefunctions of hydrogen/deuterium, or rather proton/deuteron, on the surface region of metal catalysts is therefore investigated recently in relation to the action of catalysis. It is known now that the proton on the surface of metal catalysts is not localized at a specific lattice point and also not confined on the surface but penetrated into the metal by at least one lattice distance [38], [39]. It is used even a concept "subsurface hydrogen" to express this penetration [39].

Furthermore, they use a concept of the proton band to describe the nonlocal nature of these protons [38], [39] and use a concept "hydrogen fog" in analogy to the electron gas for the nearly-free electrons in simple metals [38]. To express the penetration of protons into the metal, it is said in this paper that 'there exists another potential for hydrogen trapping between the chemisorbed and absorbed hydrogen, called the 'subsurface hydrogen.' [37 (p. 6), 39].

"It is interesting to know that the physical behavior of hydrogen isotopes in transition metals is divided into two classes; one in *bcc* metals (V, Nb, Ta etc.) and the other in *fcc* (and *hcp*) metals (Ti, Ni, Pd etc.). In the first class (*bcc* metals) a nucleus of hydrogen isotopes is localized in an interstitial site (interstice) and there are a few works to determine the profile of their wavefunctions as illustrated in Figs. 1 and 2. Accordingly, vibration and diffusion properties of these localized hydrogen isotopes have characteristics in accordance with the localization of the nuclei [5 (§3.6), 9 (§2.2),].

"On the other hand, in the second class (*fcc* and *hcp* metals), a nucleus of hydrogen isotopes is not localized at an interstitial site but extends to several interstices. And, therefore, vibration and diffusion characteristics of hydrogen isotopes are not discussed in parallel to the first class (*bcc* metals). In this class, there is no work on the wavefunctions of a proton and a deuteron in these metals suggesting difficulty to determine wavefunctions of non-localized particles (proton and deuteron)" [10 (p. 696)].

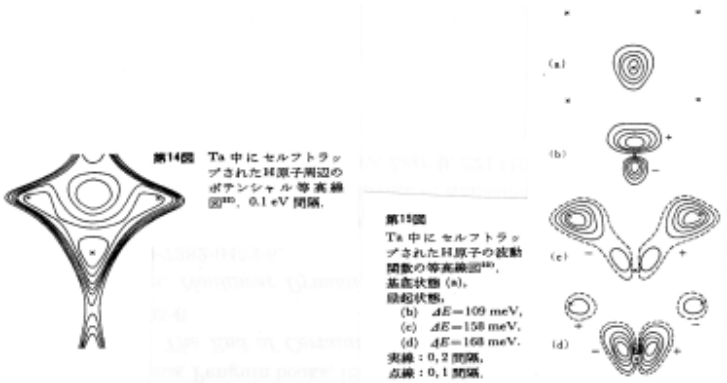

Figure 2. Localization of a hydrogen atom at an interstice in a *bcc* transition metal Ta (after Y. Fukai, *Kotai-Butsuri* (in Japanese) **16**, 253 (1981)). Left; potential contour lines around a self-trapped H-atom in Ta. Right: Contour lines of H-atom wavefunction self-trapped in Ta. From top to bottom; (a) Ground state, (b)–(d) excited states with excitation energies of ΔE = 109, 158 and 168 meV, respectively. In excited states, wavefunctions extend to the nearest lattice points and interstices." [10 (p. 695)]

We have elaborated a mechanism where the occluded hydrogen isotope with extended wavefunction interacts with several lattice nuclei through the ordinary nuclear force, thus mediating indirect interaction between these lattice nuclei [40 (Sec. 4)]. This interaction between neutrons in different lattice nuclei is the super-nuclear interaction of a new kind and results in formation of neutron bands. The neutrons in these bands expressed as the neutron Bloch waves behave as the trapped neutrons assumed in the TNCF model.

3.2. Wavefunctions of Neutrons in Lattice Nuclei

The protons and neutrons in a nucleus have been key players of nuclear physics since the discovery of the neutron in 1932 by J. Chadwick. There are several approaches for the formulation of physics of atomic nucleus, some of them referred to later are the independent-particle model and the liquid-drop model. Even after almost one century of investigation of the atomic nucleus, there remain many undetermined problems that call for thinking assumptions. Several of them will be treated in later sections.

The following treatment of atomic nuclei exemplifies the treatment of the nature of neutron wavefunctions related to CFP.

3.2.1. *Neutron Levels at Around Evaporation Level (Zero Level) [41]*

The super-nuclear interaction between lattice nuclei mediated by interstitial protons or deuterons may have a close relation to the neutron energy levels at around the evaporation levels (levels at around zero) which have wide-spread wavefunctions. The energy of neutron orbits in a nucleus with a nucleon number A calculated by C.J. Veje [41] are shown in Fig. 3 (for A = 18–210). Many examples for modification of shell structure in neutron-rich nuclei have been known recently [42]. Therefore, the energies of neutron orbits at around zero energy shown in Fig. 3 may be altered by formation of neutron-rich exotic states of relevant nuclei. We use this figure, however, for our investigation of the CFP because we have no data of up-to-date information about them at present.

"The CFP is most frequently observed in transition-metal deuterides and hydrides, especially in TiD (H), NiH (D), and PdD (H). Furthermore, these transition-metal nuclei have a common characteristic; existence of excited neutron levels near zero in an isolated nucleus, $3s_{1/2}$ in ${}^{A}_{22}$Ti ($A = 46 \sim 50$), $3s_{1/2}$ in ${}^{A}_{28}$Ni ($A = 58 \sim 64$), and $3p_{3/2}$ and $3p_{1/2}$

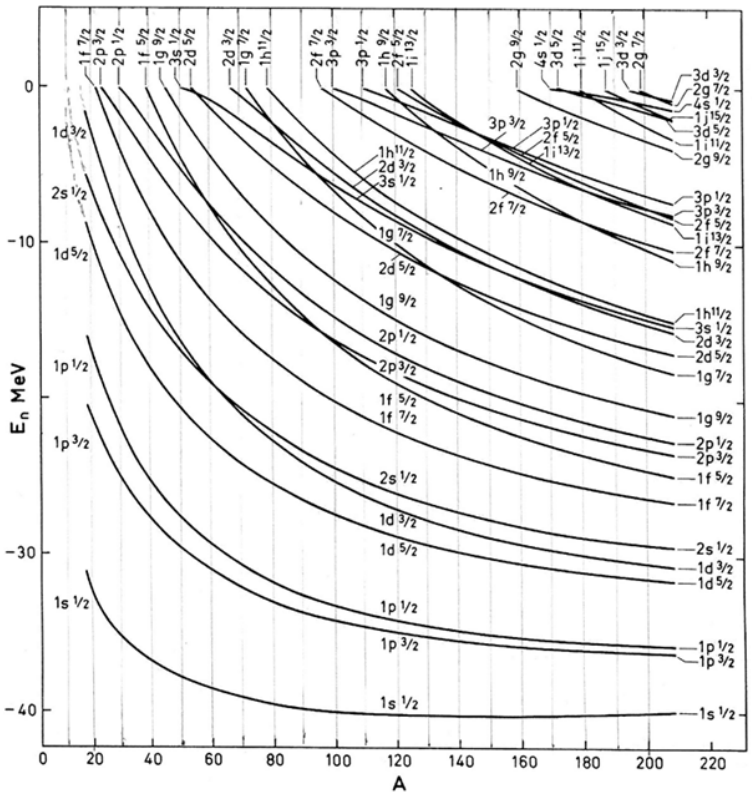

Figure 3. Energies of neutron orbits in nuclei calculated by C.J. Veje [41].

in $^{A}_{46}$Pd ($A = 102 \sim 110$) as shown in Fig. A1 [41]. As discussed in books and papers [5 (Sec. 3.6), 25] and in Secs. A3 and A4 in this Appendix, the wavefunctions of protons and deuterons in these compounds show extended nature asked for the super-nuclear interaction.

Therefore, the CFP observed in PdH (D), TiD (H) and NiH (D) is a typical illustration of the mechanism proposed by our model.

Interesting cases of XLPE ($[CH_2]_n$), CrH_x, CuH_x, ZnH_x and Al_2CuH_x are discussed successively in this Section." [40 (p. 19)].

3.2.2. *Existence of Neutron Halo States in a Nucleus at the Limit of Particle Stability [10 (pp. 693–694)]*

"—Now, there are several review articles on this problem telling following facts [43], [44]; there exist many nuclei with the so-called neutron halo extending far out of the nuclear core that is the nucleus figured out in orthodox nuclear physics. It is recognized now the necessity to treat nuclei tenderly to know their behavior in states at or near the neutron evaporation level." [10 (p. 693)].

To know the present extent of our knowledge in this field,we summarize the nuclear properties of the neutron halo closely related to the CFP from our point of view [43], [44]:

Table 1. Halo states. For each state, the excitation and separation energies and the angular momentum of the halo particle(s) are listed.

Nucleus	E_x (MeV)	S–E[a] (keV)	Configuration	l	K
^{11}Be	g.s.	504	n + ^{10}Be	0	
^{11}Be	0.32	184	n + ^{10}Be	1	
^{17}F	0.50	105	p + ^{10}O	0	
^{6}He	g.s.	973	n + n + ^{4}He		2
^{11}Li	g.s.	310	n + n + ^{9}Li		?
^{14}Be	g.s.	1340	n + n + ^{12}Be		?

[a] From Audi and Wapstra, 1993." [10 (pp. 693–694)]

1) 'Thresholds', the transition points between bound discrete states and a continuous spectrum, give rise to many fascinating phenomena. Among the newest of them are the so-called halo states that occur in some nuclei near the limit of particle stabi1ity.
2) Only very loosely bound neutrons in an *s*-state relative to the core provide an ideal halo.
3) Arbitrary large values of the mean-square radius could occur in nuclei,at least in principle.
4) If a neutron halo is defined as a divergent root-mean-square (r.m.s.) radius of the halo for the neutron separation energy S_n approaching zero,then a two-body (i.e., single-neutron) halo is possible only if the orbital angular momentum 1 = 0, l.
5) The conditions for a three-body (two neutron) halo are more restrictive and the radius is at most logarithmically divergent.
6) The known cases of even-*n* halos have the Borromean property,namely that both the two-body sub-systems (A + *n*) and (*n* + *n*) are unbound.
7) Mass calculations suggest that halo state will occur symmetrically at the neutron drip line for most elements.
8) Our knowledge is restricted to five cases in total (He, Li, Be). (Cf. Table1)
9) Halo states have unusually large nuclear and electric reaction cross sections.
10) The large size of the halo implies a narrow momentum distribution.
11) The halo neutron is in a mixed state containing its ground state and continuum states.
12) A halo neutron has a probability distribution that extends far beyond the core.
13) ^{11}Be, an example of the neutron halo size: The wave functions for the case of a single-neutron halo correspond to calculated (with Woods - Saxon potential) r.m.s. radii of the *l* = 0,1 states of 5.99 and 5.66 fm, respectively. For comparison,the r.m.s. radius of a normal *p*-shell nucleus is 2.5 fm.

Thus, we do not know yet exactly what kind of wavefunctions the halo neutrons have in the medium mass-number nuclides such as Ti, Ni and Pd. However, our knowledge about them is scarce yet, there surely exist neutrons with extended wavefunctions in lattice nuclei in CF materials.

3.3. Formation of Neutron Bands by the Super-Nuclear Interaction Between Neutrons in Different Lattice Nuclei [5, (Sec. 3.7), 9 (Sec. 2), 37].

We are able to speculate on the formation of neutron bands composed of neutrons in the outermost orbits of lattice nuclei interacting with each other through the super-nuclear interaction. The super-nuclear interaction between neutrons in adjacent lattice nuclei is formulated in our treatment of neutron-proton/deuteron interaction as an interaction mediated by protons/deuterons at interstices in the superlattice of host metals and proton/deuterons [5 (Sec. 3.7)]. We give a brief explanation of this scenario in this subsection.

Table 2. Lattice constant(s) of the metal X and the ratio l_{s-p}/a. *Lattice constant(s) (a or a and c) of X and* (l_{s-p} */a*) with l_{s-p} **(= 1000 nm)**.

X (crystal type)	***a*** or (***a*** **and** ***c***)	l_{s-p} ***/a*** (l_{s-p} ***/c***)
Ni (*fcc*)	35.2 nm	28.4
Ti (*hcp*)	29.5 and 46.9 nm	33.9 (21.3)
Pd (*fcc*)	38.9 nm	25.7

3.3.1. *Self-Organized Formation of Superlattice in Hydride Compounds [11]*

It is known that CFP is more likely to occur in CF materials with higher ratio of H/X where H is the density of hydrogen isotopes and X is the density of host elements. We noticed the self-organization of stable structures in complexity and applied this idea to the formation of the super-structure X_1H_1 from X_1H_x ($x < 1$) where the formation of the former is easier for the system with x closer to 1 [11].

The formation of superlattice of metal/hydride X_1H_1 or X_1D_1 (X = Ni, Pd, Ti, etc.) is illustrated by the following diagram:

Adsorption of H/D on the surface →
Absorption of H/D into the surface area →
Formation of a compound X_1H_x/X_1D_x ($x < 1$) →
Self-organization of X_1H_1/X_1D_1 where $x \sim 1$.

3.3.2. *Formation of Neutron Bands by the Super-Nuclear Interaction Between Neutrons in Different Lattice Nuclei [5, 9, 37]*

When a superlattice of host elements and hydrogen isotopes form, we can expect the existence of the super-nuclear interactions between neutrons in adjacent lattice nuclei [5, (Section 3.7), 9 (Section 3), 37]. We cannot make an exact calculation of the neutron bands formulated in these papers due to the scarce knowledge of wavefunctions of the relevant neutrons and protons/deuterons.

We can at most assume that the effective thickness of the self-organized surface layer of X_1H_1/X_1D_1 is as given in the next Subsection, using the knowledge of reaction products observed in several experiments.

3.3.3. *Explanation of Premises 1 and 2*

Let us consider a situation where the super-lattice XH (or XD) is formed by self-organization at the surface layer when hydrogen is absorbed from the surface of the metal. In this situation, the ratio of hydrogen/metal in the compound XH_x ($x < 1$) is higher at the surface layer than that in the volume because hydrogen is absorbed from the surface of the metal. Then, the super-lattice XH may be selectively formed by self-organization at the surface layer. The effective thickness $l_{s-p}$of the super-lattice XH where the neutron bands are formed should be fairly large compared to the lattice constants of the metal. Suggested by the experimental data telling us the nuclear transmutation in CFP occurs in the 1 μm range at the surface, we can calculate the ratio of the effective thickness l_{s-p} and a lattice constant a as tabulated in Table 3.2 for X = Ni, Ti, and Pd.

The values of l_{s-p}/a = 28.4, 33.9 and 21.3, and 25.7 for these metals in column 3 seems reasonable values for the neutron bands are formed as the pool of the trapped neutrons assumed in TNCF model.

Thickness of a super-lattice $l_{s\text{-}p}$ *is taken as about 30 times the lattice constant of* the metal X *may be enough to form the neutron band ← The observed thickness of the depth of nuclear transmutation.*

3.4. Dissipation of Excess Energy in an Excited Nucleus into Lattice Through its Interaction with Neutrons in the Neutron Bands [8]

In the phenomenological approach using the TNCF model, we have assumed that the liberated energy by the deexcitation of unstable nuclei generated in the nuclear reactions of CFP is dissipated into lattice oscillation not by photon emission (Premise 6) [3], [4], [5], [12].

We try to solve this problem using quantum mechanics as far as we can even if there is ambiguity in the relevant wavefunctions.

3.4.1. *The Problem in the Dissipation of Excitation Energy of Unstable Nuclei in CFP*

There are several expressions of the Premise 6 in our literature. The most clear-cut expression is given in the paper published in 2021 in Eqs. (8)–(10) [12].

We have written down the reactions in free space supposed by Fleischmann et al. to be responsible to their experimental results below [1], [6]:

$$d + d \rightarrow {}^{4}{}_{2}\mathrm{He}^{*} \rightarrow t\ (1.01\ \mathrm{MeV}) + p\ (3.12\ \mathrm{MeV}), \tag{1}$$

$$\rightarrow {}^{3}{}_{2}\mathrm{He}\ (0.82\ \mathrm{MeV}) + n\ (2.45\ \mathrm{MeV}), \tag{2}$$

$$\rightarrow {}^{4}{}_{2}\mathrm{He}\ (0.08\ \mathrm{MeV}) + \gamma\ (23.8\ \mathrm{MeV}). \tag{3}$$

The branching ratios of these reactions have been determined in nuclear physics as 1: 1: 10^{-7} down to low energies of a few keV.

Other nuclear reactions between light nuclei in free space are written down as follows:

$$n + p = d\ (1.3\ \mathrm{keV}) + \gamma\ (2.2\ \mathrm{MeV}), \tag{4}$$

$$n + d = t\ (6.98\ \mathrm{keV}) + \gamma\ (6.25\ \mathrm{MeV}), \tag{5}$$

$$n + {}^{6}{}_{3}\mathrm{Li} = t\ (2.7\ \mathrm{MeV}) + {}^{4}{}_{2}\mathrm{He}\ (2.1\ \mathrm{MeV}), \tag{6}$$

$$t + d = {}^{4}{}_{2}\mathrm{He}\ (3.5\ \mathrm{MeV}) + n\ (14.1\ \mathrm{MeV}). \tag{7}$$

We have given a unified explanation of CFP by the phenomenological approach using the TNCF model in which the gammas in Eqs. (3), (4) and (5) in free space are read as φ's (phonons excited by interactions of the trapped neutrons with nuclei at disordered sites) as written down below in Eqs. (8), (9) and (10) [12 (p. 3)];

$$d + d = {}^{4}{}_{2}\mathrm{He}\ (0.08\ \mathrm{MeV}) + \varphi\text{'}s\ (23.8\ \mathrm{MeV}), \tag{8}$$

$$n + p = d\ (1.3\ \mathrm{keV}) + \varphi\text{'}s\ (2.2\ \mathrm{MeV}), \tag{9}$$

$$n + d = t\ (6.98\ \mathrm{keV}) + \varphi\text{'}s\ (6.25\ \mathrm{MeV}). \tag{10}$$

As the explanation given by Blatt and Weisskopf for the deexcitation of an atom at an excited state by collisions with other atoms in a gas as shown in Appendix A1 [13 (pp. 630–631)], we can analogically understand the deexcitation processes (8), (9) and (10) as those induced by collisions of an excited nucleus with neutron Bloch waves in neutron bands formed in CF materials (see next Subsection). The formation of the neutron bands is explained by the super-nuclear interaction between neutrons in lattice nuclei which is realized by the specific overlapping of wavefunctions of occluded proton/deuteron and those of neutrons in lattice nuclei [5], [9].

3.4.2. *Deexcitation of Unstable Nuclei Isolated in Vacuum [14 (Sec. XII)]*

The deexcitation of unstable nuclei in vacuum have been investigated since the discovery of the radiation by Antoine Henri Becquerel in 1896. Especially after the establishment of the Rutherford atomic model in 1911 and discovery of the neutron by James Chadwick in 1932, the decay of unstable nuclei attracted attention of physicists from that time onwards.

One of basic investigations of the gamma-ray emission from an unstable nucleus was given by J.M. Blatt and V.F. Weisskopf (B-W) in their textbook [14]. A summary of the explanation of gamma-ray emission is given below according to the explanation by them. The essence of their theoretical treatment is given in Appendix A4-1.

Problem of wavefunctions in the unstable nuclei (independent-particle model vs. liquid-drop model) cf. Sec. 3.2 Halo states, Extended neutron wavefunctions

It is necessary to know the wavefunctions of nuclear states related to the radiative transitions. While it is not easy to know them, as B-W says in their book:

"The calculation of the radiative transition probability between two nuclear states a and b is practically impossible except in the case of deuteron. For all other nuclei, the wave functions describing the state are unknown. In spite of this,it is possible to some extent to predict the order of magnitude of the transition probabilities, since they depend very strongly on the multipole order l of the transition.

We restrict ourselves in this section to transitions between nuclear states near ground state, with energy differences less than several Mev. The wave length $\lambda/2\pi = \kappa^{-1}$ of the light is 1.97×10^{-11} cm for 1 Mev and is always large compared to nuclear dimension" [14 (p. 623)].

The wavefunctions used in the example calculation in B-W book are (1) the independent-particle picture and (2) the liquid-drop picture. Two pictures give final results with fairly distinctive characteristics:

There are characteristic differences between this expression (derived from the liquid-drop picture) and the one derived from the independent-particle picture:

(1) the matrix element is proportional to Z as a result of the fact that all charges move here in a common motion;
(2) Q contains the factor $(\hbar/\mathrm{AM}\omega)^{1/2}$ which is the matrix element of the amplitude of an oscillator vibration; hence the transition probability is proportional to ω^{2l} instead of ω^{2l+1},
(3) the nuclear radius R occurs raised to the power l–1 instead of l; finally,
(4) the electric dipole moment (l = 1) vanishes altogether. The differences can be explained by the fact that the liquid drop model and the independent-particle model represent two extreme views of nuclear dynamics. In the former model the motions of the nucleons are highly correlated; in the latter they are completely independent. [14]

The overall situation about the wavefunctions may have been improved very much since 1952 but it seems similar to that expressed in the above citation in terms of the specific nuclei we are treating in CFP as discussed in the next Subsection 3.4.3.

Finally, B-W gives a comparison of values obtained theoretical calculation and experimental observation.

"We have collected in Table 6.1 a list of some representative cases for which the nature of the radiation seemed to be established.[1] The table contains the theoretical life times of the initial states of the transitions,which are calculated from the radiative transition probabilities, (6.8) and (6.9) [calculated by the independent-particle model]. The theoretical lifetimes are compared with the experimental values.

[1]The authors are grateful to M. Deutch and M. Goldberger for their extensive help and advice in the discussion of the theoretical estimates and in the collection of data for this table. We are also grateful to W. Frauenfelder and A. de Shalit for valuable help. A much more complete table of isomeric transitions has been compiled by Goldberger (51)" [14 (p. 631)].

Table 6.1 referred to in the above sentence is cited in Appendix A4-1 as Table A4-1.

Finally, they conclude the comparison as follows:

"The electric transitions by and large show the expected behavior. The experimental lifetimes scatter considerably; they differ from the theoretical estimate (6.8) by factors up to 100. Perhaps it is significant that just among the electric quadrupole radiation one finds some transitions which are considerably faster than the theoretical estimate.

The magnetic multipole transitions agree fairly well with the estimate (6.9). In particular the magnetic transitions of multipole order $l = 4$, which constitute the best-known group of isomers,show surprisingly little deviation from the estimated values.

It is worthwhile to remark that the liquid drop model estimate (6.10) would lead to much poorer agreement with the experimental lifetime" [14 (pp. 631, 633, 634)].

3.4.3. *Formulation of the Deexcitation of an Unstable Nucleus Interacting with Neutrons in a Neutron Band*

Let us consider the way we describe (1) wavefunctions of relevant particles and (2) the interaction potential between nucleons in the unstable nucleus ${}^{A}_{Z}\mathrm{X}^{*}$ and the neutron Bloch waves in a neutron band. It is possible to formally describe the deexcitation probability of the unstable nuclei ${}^{A}_{Z}X^{*}$ interacting with neutron Bloch waves to ${}^{A}_{Z}\mathrm{X}$ giving the excess energy ε to neutrons even if quantitative calculation is far more out of our power considering the difficulty of the "simple" calculation of the probability of

$$ {}^{A}_{Z}X * to {}^{A}_{Z}X + \gamma $$

given by B-W in the previous subsection 3.4.2.

This is a reason that we have to depend on the analogy explained in the next Subsection.

3.4.4. *Qualitative Explanation of Dissipation of Excess Energy from Unstable Nuclei to Lattice by Analogy to the Atomic Deexcitation Used by J.M. Blatt and V.F. Weisskopf [14 (Appendix A4-2)]*

We try to understand the Premise 6 by analogy to the atomic deexcitation described by B-W [14 (Appendix A4-2)].

They discussed the atomic deexcitation by collisions with other atoms as follows:

"*An atom in one of these states can lose its excitation by non-radiative collisions with other atoms. Thus, the mean lifetime between collisions provides an upper limit for atomic life-times. Radiative transitions which by themselves would lead longer lifetimes have to compete with the collision process and are correspondingly weak and hard to observe"* ([14 (pp. 630–631)].

We are able to use the analogy of complexity mentioned by Dr. Y. Yoshinaga [45], a mathematician, to conclude the possible dissipation of an unstable nucleus to the lattice through the interaction of the nucleus and the neutron Bloch waves in the neutron bands.

"*On the one hand, the science of complex systems seeks to uncover the simplicity that lies deep within complexity. At the same time, it starts from a thorough reflection on simple elemental reductionist thinking. On the one hand, it is a constructive science that seeks to find the key to unlocking the mysteries of complexity in the virtual world inside computers. On the other hand, it is also a science that considers that complex phenomena are always already there, as a presence that cannot be discarded, prior to scientific analysis. On the one hand, it is an ambition to establish a new scientific methodology, but on the other hand, it gives a significant role to analogy, which has traditionally been excluded from scientific thinking*." (translation assisted by *Google translation*) [45 (p. 237)].

"The deexcitation of an unstable atom by non-radiative collisions with other atoms" described in the B-W sentence cited above can be used for "the deexcitation of an unstable nucleus by non-radiative interaction with neutron Bloch waves." The dissipated energy to the neutron Bloch waves can be transferred to lattice vibrations closely related with the neutron Bloch waves."

The deexcitation of the unstable nucleus through the interaction with neutron Bloch waves is investigated rather quantitively in Appendix A5.

4. Conclusion

The science of the cold fusion phenomenon (CFP) has been in the process of formation for about 35 years, which is not a brief period.

We can compare this period to the period 13 years of quantum mechanics from the proposal of the Bohr model of atoms in 1913 to the proposal of the Heisenberg and the Schroedinger formulations of quantum mechanics in 1926. This difference in the formations of quantum mechanics and the science of CFP depends definitely on the different complexity in the two phenomena, one in atoms composed of a nucleus and electrons interacting with electromagnetic force and another in solids composed of transition metals (and other elements, carbon) and hydrogen isotopes.

The state composed of lattice nuclei and occluded (or included) protons/deuterons as explained in Sec. 3 in this paper remind us of the Coulomb lattice of "clusters of neutrons, protons and compensating electrons" worked out by J.W. Negele and D. Vautherin [46] in their calculation of the neutron star matter [5 (Sec. 3.7.3)]. Considering the similarity of (1) the Coulomb lattice of Negele et al. [46] and the formation of the neutron bands containing neutron Bloch waves in them explained in Sec. 3.3 and (2) the neutron drops formed by the band neutrons in between the lattice nuclei [5 (Sec. 3.7.6)], we understand that the CFP is essentially the many-body problem and should not be easily considered solvable by a single-particle approach such as the *d–d* fusion reactions supposed to be the mechanism for the excess heat generation.

There is another important new factor we have to note in the science of the CFP. As we have surveyed in this paper, there is a new element, complexity, which has not existed in the science of atoms heretofore. This element prevented simple expansion of the logic we have successfully used in solid state physics and nuclear physics. Due to this new element, we have to depend on the phenomenological approach using a model based on experimental facts, even if it contains premises which do not fit with existing common sense of science which has been successful in physics of simple systems for a very long time.

Complexity is a new science developed over the last 50 years. It includes alien ideas not used in the science of simple systems composed of elements interacting with linear force. One of the most extraordinary is the analogy as Y. Yoshinaga mentioned as follows:

"*On the one hand, it is an ambition to establish a new scientific methodology, but on the other hand, it gives a significant role to analogy, which has traditionally been excluded from scientific thinking*." [45 (p. 237)]

In this paper, we have tried to present the overall picture of our phenomenological endeavor in a unified form to obtain rigorous evaluation from readers for the advancement of this science. We hope that this paper will be useful for readers and contribute to the advancement of the science of CFP.

Appendices

A1. Impacts of a Phenomenological Model [4]
A2. Premises of the TNCF model [4]
A3. Non-localized Wavefunctions of Hydrogen in *fcc* Transition Metals
A4. Interaction of Nuclei with Electromagnetic Radiation ([13])
A5. De-excitation of an Unstable Nucleus through Interaction with Neutron Bloch Waves

A1. Bohr's Model of Atoms and Impacts of a Phenomenological Model [4 (Sec. 10.4)]

A1-1. Bohr's Model of Atoms [4 (Sec. 10.3)]

"In the study of a complex phenomenon as cold fusion, it will be advisable to recollect famous models which played important roles in the history of physics.

10.3a. Bohr model of atoms.

The most famous model in the atomic physics is "the Bohr model" of atoms proposed in 1913 by N. Bohr to explain paradox of their finite volume and atomic spectra difficult to understand by the classical electrodynamics: The old theory had told that;

(1) the electron in an atom accelerated by the nucleus lose energy emitting radiation and shrink to zero volume in contradiction with finite volume of the atoms well established by daily experience and
(2) the emitted radiation has a continuous spectrum corresponding to the frequency of its orbital motion, but sharp line spectrum observed.

To explain these experimental facts, N. Bohr settled four postulates contradicting classical electrodynamics. Following explanation is from *Encyclopedia Britannica,* Vol. 2, p. 710 (1963):

'In these terms the postulates of Bohr's theory can be stated as follows:

1. Electrons can move in circular orbits around the atomic nucleus.
2. The only orbits possible are those for which the orbital angular momentum is an integral multiple of $h/2\pi$, where h is the Planck's constant.
3. Those orbits are "stationary" in the sense that so long as an electron remains in a given orbit it radiates no energy.
4. An electron may jump from one orbit to a second orbit of lower (more negative) energy, closer to the nucleus; in this process the energy liberated is emitted as a single quantum of light.

The arbitrariness of these postulates was admitted, but their success was beyond dispute. Later the new atomic mechanics – called wave mechanics or quantum mechanics – led to the same results in a less forced manner.' (A.P. French, *Encyclopedia Britannica,* Vol. 2, p. 710 (1963))" [4 (Sec. 10.3)]

A1-2. Impacts of a Phenomenological Model [4 (Sec. 10.4)]

"10.4 Impacts of the Phenomenological Theory

As shown in the preceding section, the phenomenological theory uses sometimes the most fantastic ideas to explain phenomenon otherwise difficult to explain. Therefore, there appeared strong counter reaction to those models from people trapped in the conventional frame of science at that time.

There are several proofs of this kind recorded in memoirs and diaries of scientists who made great contributions to science before or after the controversial period of Bohr's model. The following are some of them provided by Prof. S. Nishio of Nihon University (History of Science).

A Nobel prize laureate Dr. J.J. Thomson (in 1906) who discovered the electron and also proposed an atomic model with a structure like a watermelon (its electrons as seeds and positive charge as flesh) responded as follows (not literally);

"The stationary states of electron in the atom assumed in Bohr's theory is in contradiction with the classical electrodynamics. Furthermore, it is undetermined that Coulomb's law of electric force is applicable to such a small range as in the atom. Therefore, it is nonsense to consider such model to explain phenomena related with atoms."

P. Ehrenfest born in Austria had studied in Holland as a Professor of Leiden University at the time when the Bohr's model was proposed. Attacked by the impact of Bohr's model, he wrote a letter to his friend H.A. Lorentz in August 1913:[131]

"Bohr's work on the quantum theory of the Balmer formula (in the *Phil. Mag*.), has driven me to despair. If this is the way to reach the goal, I must give up doing physics."

However, "Once he met Bohr and absorbed the essence of his ideas and attitudes in direct conversation, Ehrenfest became an enthusiastic boost and close friend, but that had to wait for the end of the World War."

His most famous work may be "the Ehrenfest's theorem" stating that a quantum-mechanical wave packet obeys the equations of motion of the corresponding classical particle when the position, momentum, and force acting on the particle are replaced by the expectation values of these quantities.

E. Schroedinger had to say about the frequency condition of Bohr's, major objection was on this point at that time, in 1926:[131]

"The frequency discrepancy in the Bohr model, on the other hand, seems to me, (and had indeed seemed to me since 1914), to be something so *monstrous,* that I should like to characterize the excitation of light in this way as really almost *inconceivable*."

On the other hand, A. Einstein was affirmative to Bohr's model. His reaction is recorded in C. Hevesy's letter:[131]

"Then the frequency of the light does not depend at all on the frequency of the electron. And this is an *enormous achievement*. The theory of Bohr must be right then.

The examples of famous models in history illustrated above in this Chapter clearly show the essential character of the model in science: The value of a model is determined only by its power in explaining facts irrespective of validity of its premises in the conventional science. The meaning of the premises could be elucidated by the following works establishing a new paradigm, in the meaning used by T. Kuhn.[133]

[131]M. Klein, *Paul Ehrenfest*, pp. 278–279. North Holland, Amsterdam, 1970.

[133]T. Kuhn, *The Structure of Scientific Revolution*, 2^{nd} ed., University of Chicago Press, Chicago, USA, 1970." [4 (Sec. 10.4)]

A2. Premises of the TNCF model [4 (Sec. 11.1a)]

"11.1a Premises of the TNCF Model

The TNCF model is a phenomenological one and the basic premises (assumptions) extracted from experimental data sets are summarized as follows: [241,255,266,274]

Premise 1.

tWe assume the *a priori* existence of the quasi-stable trapped neutron with a density n_n in pertinent solids, to which the neutron is supplied from the ambient neutron at first and then by breeding processes (explained below) in the sample.

The density n_n is an adjustable parameter in the TNCF model which will be determined by an experimental data set using the supplementary premises which will be explained below concerning reactions of the trapped neutron with other particles in the solids. The quasi-stability of the trapped neutron means that the neutron trapped in the crystal does not decay until a strong perturbation destroys the stability while a free neutron decays with a time constant of 887.4 ± 0.7 s.

Premise 2.

The trapped neutron in a solid reacts with another nucleus in the surface layer of the solid, where it suffers a strong perturbation, as if they are in vacuum. We express this property by taking the parameter (the instability parameter) ξ, defined in the relation (11.1) written down below, as $\xi = 1$.

We have to mention here that the instability parameter ξ in the surface layer is not known, and it might be, as noticed recently, more than one ($1 < \xi$) making the determined value of the parameter n_n smaller. This ambiguity is suggested by various anomalous changes of decay character of radioactive isotopes and by unexpected fission products in the surface layer.

Premise 3.
The trapped neutron reacts with another perturbing nucleus in volume by a reaction rate given in the relation (11.1) below with a value of the instability parameter $\xi < 0.01$ due to its stability in the volume (except in special situations such as at extremely elevated temperature such as 3000 K).

The following premises on the measured quantities of nuclear products and the excess heat are used to calculate reaction rates, for simplicity:

Premise 4.
Product nuclei of a reaction lose all their kinetic energy in the sample except when they go out without energy loss.

Premise 5.
A nuclear product observed outside of the sample has the same energy as its initial (or original) one.

This means that if an energy spectrum of a gamma-ray photon or neutron is observed outside, it reflects directly nuclear reactions in the solid sample. The same is for the distribution of the transmuted nucleus in the sample. Those spectra and the distributions of the transmuted nuclei are the direct information from the individual events of the nuclear reaction in the sample.

Premise 6.
The amount of the excess heat is the total liberated energy in nuclear reactions dissipated in the sample except that brought out by nuclear products observed outside.

Premise 7.
Tritium and helium measured in a system are accepted as all of them generated in the sample.

The amounts of the excess heat, tritium and helium are accumulated quantities reflecting nuclear reactions in the sample indirectly and are the indirect information from the individual events.

Premises about structure of the sample are expressed as follows:

Premise 8.
In electrolytic experiments, the thickness l of the alkali metal layer on the cathode surface (surface layer) will be taken as $l = 1$ μm (though the experimental evidence shows that it is $l \sim 10$ μm).

Premise 9.
The mean free path or path length l_t of the triton with an energy 2.7 MeV generated by

$n + {}^6\mathrm{Li}$ fusion reaction will be taken as $l_t = 1$ μm irrespective of material of the solid. Collision and fusion cross sections of the triton with nuclei in the sample will be taken as the same as those in vacuum.

Premise 10.
Efficiency of detectors will be assumed as 100% except otherwise described, i.e., the observed quantities are the same as those generated in the sample and to be observed by the detector in experiments if there is no description of its efficiency.

A premise will be made to calculate the number of events N_Q producing the excess heat Q.

Premise 11.
In the calculation of the number of an event (a nuclear reaction) N_Q producing the excess heat Q, the average energy liberated in the reactions is assumed as 5 MeV unless the reaction is identified:

$$N_Q = \text{Excess heat } Q \text{ (MeV)/ 5 (MeV)}.$$

If the stability of the trapped neutron is lost by a large perturbation in the surface layer or in the volume, the number of trigger reactions (per unit time) between trapped thermal neutrons and a nucleus ${}^{A}_{Z}\mathrm{M}$ may be calculated by the same formula as the usual collision process in vacuum but an instability parameter ξ:

$$P_f = 0.35\, n_n v_n n_M V \sigma_{nM} \xi, \tag{11.1}$$

where $0.35 n_n v_n$ is the flow density of the trapped thermal neutron per unit area and time, n_M is the density of the nucleus, V is the volume where the reaction occurs, σ_{nM} is the cross section of the reaction. The instability parameter ξ as taken into the relation (11.1) expresses an order of the stability of the trapped neutron in the region as explained in premises 2 and 3, and also in the next paragraph.

In the electrolytic experiments, we have taken $\xi = 1$ in the surface layer and $\xi = 0$ in the volume except otherwise stated (Premises 2 and 3). The values of $\xi = 0.01$ instead of $\xi = 0$ in the relation (11.1) will result in lower n_n in the electrolytic data by a factor 2 than that determined with a value $\xi = 0$ as had been used in our former analyses. (In this Chapter, we will cite previous results with $\xi = 0$ as they were.)

In the case of a sample with a definite boundary layer surrounding a trapping region where the thermal neutron the volume V should be that of the boundary region where the nucleus reacts with the thermal neutron. On the other hand, in a sample without a definite boundary layer but a disordered array of minority species of lattice nuclei in the sample, the volume should be the whole volume of the sample.

If a fusion reaction occurs between a trapped thermal neutron and one of lattice nuclei ${}^{A}_{Z}\mathrm{M}$ with a mass number A and an atomic number Z, there appears an excess energy Q and nuclear products as follows:

$$n + {}^{A}_{Z}\mathrm{M} = {}^{A+1-b}_{Z-a}\mathrm{M'} + {}^{b}_{a}\mathrm{M''} + Q,$$

where ${}^{0}_{0}\mathrm{M} \equiv \gamma$, ${}^{1}_{0}\mathrm{M} \equiv n$, ${}^{1}_{1}\mathrm{M} \equiv p$, ${}^{2}_{1}\mathrm{M} \equiv d$, ${}^{3}_{1}\mathrm{M} \equiv t$, ${}^{4}_{2}\mathrm{M} \equiv {}^{4}\mathrm{He}$, etc." [4 (Sec. 11.1a)].

A3. Non-Localized Wavefunctions of Hydrogen in fcc Transition Metals

A3-1. Hydrogen Isotopes in fcc Transition Metals [10 (Sec. 2.2)]

"The behavior of hydrogen isotopes in transition metals has been investigated for more than 100 years and there are abundant data on diffusion and vibration characteristics of protons and deuterons in them. Several interesting features are introduced here from our point of view in relation to CFP.

There are two groups of metals in which H diffusion has been measured (Sussmann 1972). The first consists of Nb,V and Ta and the second consists of Ni,Pd,and Ti. Sussmann et al. excluded the second group from their treatment "because the potential felt in them by the hydrogen is very different from sinusoidal," which is in the first group. This is an expression showing the difference of physics of diffusion in the former *bcc* transition metals and the latter *fcc* (*hcp*) ones.

Springer (Springer 1978) explains some peculiar properties of Pd deuterides compared with hydrides. "In the *fcc* palladium lattice,hydrogen or deuterium atoms occupy octahedral sites.... The zone center frequency (in $PdH_{0.63}$) is more than two times lower than it is in the case of NbD_x which implies a weak Pd-D interaction." "The pronounced maximum appearing in the longitudinal optic branch indicates strong second neighbor D-D interactions whose strength is comparable to the first neighbor D-D interaction."

There are contradicting facts about physical properties of Pd-H systems: In low-density samples (i.e., H/Pd ratio ~ 0) where diffusion experiments were usually performed,H is in low energy states showing large values of activation energy for self-diffusion. In high-density samples (i.e., H/Pd ratio ~ 1 where elastic measurement was usually performed) H-Pd interaction is comparable to H-H interaction even if H-Pd distance (2.03 A) is 1ess than that of H-H ($\sqrt{2}$ x 2.03 A) and the large value of the nuclear charge Z = 46 of Pd.

The latter fact probably reflects the nuclear interaction between a proton and Pd nucleus,which is attractive as we can guess from nuclear property of Pd isotopes discussed in Section 2.3-1.

Puska (Puska 1984) further explains the difference between *fcc* and *bcc* transition metals about hydrogen diffusion. "Our results suggest a diffusion model for hydrogen in *fcc* metals that is different from the one described for *bcc* metals. First, we note that in the high-temperature region the diffusion activation in *fcc* metals is typically 0.2–0.4 eV, which is much more than the calculated self-trapping energies in the octahedral sites. On the other hand, according to calculations, *self-trapping in the tetrahedral sites is unprovable, and thus hydrogen would not be localized at the tetrahedral site during the activation process, but its wave function should be spread several interstices . . .*"

The behavior of proton in the tetrahedral site reminds us of proton conductors that also show CFP as tabulated in Table 1 (Chapter 1).

Furthermore, there is a peculiarity of elastic properties in PdH and PdD. Wicke (Wicke 1978) explains strange character of interactions in them: "Consequently, Burch introduced the idea of a repulsion of H atoms on next-nearest neighbor sites,which would overcompensate the attraction of nearest neighbor H atoms at high concentrations."

Characteristics of CFP tabulated in Table 1 show another difference in properties of *fcc* transition metals and *bcc* ones. From our point of view, these characteristics of *fcc* transition metals should have interrelation among them" [9 (Sec. 2.2)].

A3-2 Wavefunctions of Protons/Deuterons in Transition-Metal Hydrides and Deuterides

"On the other hand, in the second class (*fcc* and *hcp* metals), a nucleus of hydrogen isotopes is not localized at an interstitial site but extends to several interstices." [5(§3.6), 9(§2.2)]. And, therefore, vibration and diffusion characteristics of hydrogen isotopes are not discussed in parallel to the first class (*bcc* metals). In this class, there is no work on the wavefunctions of a proton and a deuteron in these metals suggesting difficulty to determine wavefunctions of non-localized particles (proton and deuteron).

In relation to the occurrence of the super-nuclear interaction proposed by us [5(§3.7.2), 9(§3)], we have to estimate the wavefunction $\Phi(\boldsymbol{R}; \mathbf{b}_j)$ of interstitial proton (or deuteron) at around a nearest neighbor lattice nucleus. The super-nuclear interaction determines the width of the neutron band and then the neutron density at a boundary/surface region. The latter is related to the CF matter that interacts especially with adsorbed or absorbed nuclei and also with lattice nuclei at the boundary/surface region.

We have formulated this scenario in the frame of the second-order perturbation theory [5], [9]. On the same line described in these publications, we discuss here a possibility to determine the proton/deuteron wavefunction in terms of the data obtained in the CFP research. [10 (Sec. 2.2)]

A4. Interaction of Nuclei with Electromagnetic Radiation ([14])

A basic treatment of the gamma decay had been given by Blatt and Weiskopf in their textbook published in 1952 [14]. They have given standard treatment for this problem using materials obtained at the time. We can use their fundamental ideas to discuss the problem we are trying to deal with.

A4-1 Test of the Lifetime Estimates [14 (Chapter XII)]

"p. 624

We have estimated the kinetic energy per nucleon in Chapter VII,Section VII, Section 2, to be of the order of 10 to 20 Mev. We get an estimate for $(v/c)^2$ by comparing this kinetic energy with the rest energy Mc^2 of the nucleons. Thus $(v/c)^2$ is of the order 0.02 to 0.04.

pp. 625–626

In order to obtain an estimate of the actual value of the multipole moments we must adopt some kind of nuclear model. The simplest results can be drawn from the independent-particle model, and there are experimental indications (see Chapter XIV) that this model describes low-lying nuclear levels reasonably well. In the independent-particle model a state of the nucleus is described by the quantum numbers of the individual nucleons. The multipole moments, (3.32) to (3.35), between two nuclear states *a* and *b* are different from zero only if the two states differ in the quantum numbers of only one nucleon. If *a* and *b* differed in the quantum numbers of two nucleons, all integrals would vanish for orthogonality reasons, since the operators in the integrals contain the coordinates of only one nucleon at a time.

Then the two wave functions of the proton have the form

$$\mathrm{w}_a = u_a(r)\ \mathrm{Y}_{\mathrm{lm}}(\theta,\varphi)\alpha \tag{6.5}$$
$$\mathrm{w}_b = u_b(r)\ (4\pi)^{-1/2}\alpha$$

where α is the spin function for a particle with spin up, and u_a and u_b are function of $r = |\mathrm{r}|$ only. Substitution into (3.32) gives (remembering that only the first term of the sum over k contribute)

$$Q_{lm} = (4\pi)^{-1/2} l\ J_1 \text{ (independent-particle model)}, \tag{6.6}$$

where

$$J_l = \int_0^\infty r^l u_a(r) u_b(r) r^2 dr. \tag{6.7}$$

We now proceed to estimate the order of magnitude of this radial integral. The simplest estimate is obtained by both $u_a(r)$ and $u_b(r)$ equal to the same constant for values of *r* less than the nuclear radius *R*,and equal to zero for values of *r* greater than *R*. The constant is found from the normalization of the wave functions $w_a$and w_b and is $(3/\mathrm{R}^3)^{1/2}$.

With this assumption we get the order-of-magnitude estimate

$$J_l \sim 3\mathrm{R}^l/(l+3) \tag{6.7a}$$

Evidently (6.7a) is a very rough estimate. The radial wave functions $u_a(r)$ and $u_b(\ r)$ are not constant but oscillate in some manner for $r < R$ and drop gradually to zero for $r > R$. We therefore can expect that the actual value of J_l is smaller than (6.7a). The estimate (6.7a) gives an idea of the order of magnitude which one can anticipate in most transition between low-lying levels. Values of J_l smaller than (6.7a) by factors, say,up to 30 may well be expected.

pp. 626–627

If we substitute estimates (6.7a), (6.6), and (6.3a) for the multipole moments into the expressions (3.21) and (3.22) for the transition probabilities, we get the following expression for *electric radiation of multipole order l*,[1]

$$\begin{aligned} T_E(l) &\approx \{2(l+1)/l[(2l+1)!!]^2\}(3/(l+3))^2(e^2/\hbar c)(\kappa R)^{2l}\omega \\ &= \{4.4(l+1)/l[(2l+1)!!]^2\}(3/(l+3))^2(\hbar\omega/197\ \mathrm{Mev})^{2l+1} \times (R \text{ in } 10^{-13}\mathrm{cm})2l10^{21}\mathrm{cm}^{-1} \end{aligned} \tag{6.8}$$

and, for *magnetic radiation of multipole order l*,

$$\begin{aligned} T_M(l) &\approx \{20(\mathrm{l}+1)/l[(2l+1)!!]^2\}(3/(l+3))^2(\mathrm{e}^2/\hbar\ \mathrm{c})(\hbar/McR)^2\ (\kappa\mathrm{R})^{2l}\omega \\ &= \{1.9(\mathrm{l}+1)/\ l[(2l+1)!!]^2\}(3/(l+3))^2(\hbar\omega/197\ \mathrm{Mev})^{2l+1}\ \mathrm{x}\ (R \text{ in } 10^{-13}\ \mathrm{cm})^{2l-2}\ 10^{21}\mathrm{cm}^{-1} \end{aligned} \tag{6.9}$$

Table 3. Test of the Lifetime Estimates, (6.8) and (6.9).

Nucleus	$\hbar\omega$	α_K	K/L	J_i	J_f	Type	Lifetime Theory	experiment	$\left(\frac{\text{Theory}}{\text{Exp.}}\right)$
A. Electric Transitions									
N^{13}	2.38	...	...	$\frac{1}{2},+$	$\frac{1}{2},-$	E1	$7(-17)$	$1(-15)$	0.07
Cd^{111}	0.247	0.054	5.2	$\frac{1}{2},+$	$\frac{1}{2}$	E2	$1(-8)$	$8(-8)$	0.1
Os^{186}	0.137	0.35	0.6	2	0	E2	$5(-8)$	$8(-10)$	65
Hg^{197}	0.133	~ 0.53	0.3	...	...	E2	$3(-8)$	$7(-9)$	5
Hg^{198}	0.411	0.031	...	...	...	E2	$4(-10)$	$\leq 5(-11)$	≥ 8
In^{114}	0.192	2	1	...	...	E4	3(4)	4(6)	0.008
Pb^{204}	0.905	0.06	1.5	...	...	E5	3(3)	4(3)	0.8
B. Magnetic Transitions									
Li^7	0.478	...	...	$\frac{1}{2},-$	$\frac{3}{2},-$	M1	$2(-13)$	$8(-14)$	3
In^{118}	0.39	0.6	5.4	...	$\frac{3}{2}$	M4	2(4)	6(3)	3
In^{115}	0.338	~ 1	5	...	$\frac{3}{2}$	M4	6(4)	2(4)	3
Xe^{181}	0.163	~ 20	2.34	...	2	M4	2 (6)	1(7)	0.2
Ba^{188}	0.276	2.4	3.2	...	...	M4	1 (5)	1(5)	1
Ba^{177}	0.663	0.097	4.8	...	...	M4	2(2)	2(2)	1

Equations (6.8) and (6.9) [obtained by the single-particle model] are only very rough estimates. The actual values are expected to be smaller than these estimates by factors perhaps up to 1000. Exceptional cases of transitions between two states whose wavefunctions overlap very badly cannot be excluded; in those cases the actual transition probabilities would be very much smaller than the predicted ones (by factors much larger than 10^3). Still these estimates may be of some value for a first orientation since,for gamma-ray energies below 1 Mev,$T_E(l)$ as well as $T_M(l)$ changes by a factor of about 10^6 when l changes by one unit. Expression (6.8) for the electric transition probability can be considered an upper limit as long as the independent-particle model is applicable.

These estimates refer to the transition probability associated with emission of multipole radiation. To get the actual lifetimes we must correct for the transition probability associated with the internal conversion process, i.e., multiply by $(1 + \alpha)$, where α is the conversion coefficient. This correction is very important for $\hbar\omega$ in the 100-kev region and medium or heavy elements,especially for high multipole orders l (Axel 49). In many cases the internal conversion coefficient is known known experimentally, so that the correction coefficient is known experimentally, so that the correction can be made without knowing the multipole order and parity of the transition.

The first column lists the nucleus in which the gamma-ray transition occurs, the second column gives the energy of the gamma-ray, in Mev; the next four column list the data used for the multipole determination: the K shell conversion coefficient α_K, the ratio of K shell to L shell conversion, the spins J_i of the initial and J_f of the final state of the nucleus. Column 7 lists the multipole type and order; the notation used is E3 for an electric transition of multipole order *l*= 3, M4 for a magnetic transition of multipole order l = 4, etc. Columns 8 and 9 give the theoretical and experimental values of the half-lives; 7(–17) means 7×10^{-17} sec; the theoretical values are computed from (6.8) and (6.9), with the correction for internal conversion made as far as possible by use of experimentally determined conversion coefficients; the nuclear radius was assumed to be $R = 1.4A^{1/3} \times 10^{-13}$ cm; most of the numbers are rounded off to one significant digit. The last column gives the ratio of theoretical to the experimental lifetime in each case. For sources, see the footnote.

[1](**Footnote**)

The data for the multipole determination and the lifetime were taken mainly from the compilation of nuclear data by K. Way (50). In addition, the following references were employed: N^{13}: Hornyak 50. Fowler 49, Thomas 50, 51a. The identification of the multipole order is unique since the pair conversion has been measured for the mirror transition in C^{13}. The assignment 1/2 to the initial state comes from the measured proton width of this (compound) state. A detailed calculation of the theoretical lifetime which uses reasonable wavefunctions for the protons in the initial and final states gives much better agreement between the theoretical and experimental values than (6.8). Cd^{111}: Roberts 51, McGinnis 51, and a private communication from M. Goldhaber. Os^{186}: Metzger 51, McGowan, 50,51. Hg^{191}:Frauenfelder 50,Huber 51. Hg^{198}: R. E. Bell, private communication. Li^{7}: Hornyak 50, Elliot 48, 49, Rose 50, Littauer 50; the assignment of equal parities to the two states is required by the K-capture branching ratio of Be^{7}. In^{114}; Steffen 51. In^{115}: Bell 49; the beta decay data give some information about the spin of the initial state. Be^{137}: Waggoner 50a." [13 (Chapter XII)].

A4-2. Why are no Long-Lived Isomeric Electronic States Observed in Atoms Under Laboratory Conditions?

If there is some chance of nuclear interaction between excited nuclei and other particles X's, for instance neutrons, the excited nuclei can lose its excitation energy by non-radiative collisions with X's. We can cite an idea for the deexcitation of an excited atom by collisions with other atoms from a book by J.M. Blatt and V.F. Weisskopf [14 (pp. 630–631)] [Blatt 1952 (pp. 630–631)]:

"*We may ask why no long-lived isomeric electronic states are observed in atoms under laboratory conditions. There are many atomic states which can lose their excitation only by emission of radiation of higher multipole order than the usual atomic radiations (electric dipole). However,under laboratory conditions the atoms are not isolated from each other but collide frequently with each other,the mean time between collisions depending on the pressure. An atom in one of these states can lose its excitation by non-radiative collisions with other atoms. Thus the mean lifetime between collisions provides an upper limit for atomic life-times. Radiative transitions which by themselves would lead longer lifetimes have to compete with the collision process and are correspondingly weak and hard to observe. These highly forbidden lines show up more strongly in the spectra of some stars and nebulae. The pressures there are much less than the best vacuum attainable on earth, and the mean time between collisions of atoms is correspondingly much longer. In the nuclear case the collisions between nuclei are completely unimportant since the nuclei are shielded from each other by their electron clouds and would in any case repel each other electrostatically if brought close together. The non-radiative de-excitation of nuclei is confined to the internal conversion process*." [14 (pp. 630–631)].

This idea of "the atomic deexcitation by atomic collisions" gives a hint of an explanation of "the deexcitation of unstable nuclei generated by nuclear reactions in CFP" discussed in Section 3.2. If there are some chance of nuclear interaction between excited nuclei and neutrons in the neutron bands, the excitation energy of the excited nuclei is absorbed by the neutrons and finally handed over phonons [φ's in Eqs. (8)–(9)]. This is the story that the excited nuclei can lose its excitation by non-radiative collisions with band neutrons to excite phonons of the lattice.

A5. De-excitation of Unstable Nucleus through Interaction with Neutron Bloch Waves

There are many examples of (1) the de-excitation of unstable nuclei without emission of gamma photons and (2) huge decay time reductions of radioactive nuclei in the CFP [4 (Secs. 9 and 11), 5 (Secs. 2.5 and 2.10), 6 (Appendix C), 12 (Secs. 4 and 5)].

It is a common sense in nuclear physics that the nuclear processes in a nucleus of a size in the range of femtometer are not influenced at all by outer charged particles in the energy range of less than 1 keV. This is the reason we used our phenomenological approach, the TNCF model based on the quasi-stable neutrons in the CF materials, to give a consistent explanation for the enormous and various experimental facts obtained in the CFP [4], [5], [6], [12].

In this Appendix A5, we pick up several typical events related to the unbelievable facts of the changes of stabilization characteristics of unstable nuclei in the CFP which have betrayed the common sense of nuclear physics, i.e., changes of decay characteristics in the CF materials.

A5-1. De-excitation of Unstable Nucleus without Emission of γ-Photon in the CFP by Interaction with Neutron Bloch Wave

There are many examples showing stabilization of nuclei (e.g. ${}^{A}_{Z}\mathrm{X}$) appeared in the CF materials after events producing enormous huge excess heat. In the reasonable explanation of the events from the original nuclei in the initial state to the final result, we have to assume the nucleus ${}^{A}_{Z}\mathrm{X}$ originally in the excited state ${}^{A}_{Z}\mathrm{X}^{*}$ and stabilized to ${}^{A}_{Z}\mathrm{X}$ emitting a γ-photon in vacuum while in the CFP we have seldom observed the γ-photon [4 (Sec. 9.1), 5 (Sec. 2.10)].

We cite only one example in this Subsection showing clearly the absence of γ-photons in stabilization of ${}^{11}{}_{5}\mathrm{B}^{*}$ resulted by the reaction $n + {}^{10}{}_{5}\mathrm{B} \rightarrow {}^{11}{}_{5}\mathrm{B}^{*}$ in our scheme.

A5-1-1. Depletion of ${}^{10}{}_{5}\mathrm{B}$.

T.O. Passell observed depletion of ${}^{10}{}_{5}\mathrm{B}$ in Pd cathode which produced excess heat [47], [48]. These papers compare measurements on cathodes that successfully produced excess heat with the same measurements on virgin material from the same batch of palladium. Significant depletion of the B-10 isotope has been observed in a number of cathodes relative to that in the virgin material.

We will take up this work in Sec. A5-4 to investigate a possible quantum mechanical mechanism of deexcitation of unstable nuclei by interaction with neutron Bloch waves.

A5-2. Decay Time Reduction of α and β Decay in the CFP by Interaction with Neutron Bloch Wave

There are very many observations of huge reduction of decay constants of radioactive nuclei in the CFP [4 (Sec. 9.1), 5 (Sec. 2.5.1.1), 49 (Secs. 6.3 and 6.4)]. We take up a few examples from them and discuss one by Dash et al. [50], [51] which we did not analyze before.

A5-2-1. Reduction of decay constant of the unstable nucleus ${}^{7}{}_{3}\mathrm{Li}^{*}$.

Morrey et al. [52] measured ${}^{4}{}_{2}\mathrm{He}$ in the electrolytic system Pd/$\mathrm{D_2O}$ + electrolytes/Pt used by Fleischmann et al. [1]. We have analyzed their data [53] using the TNCF model. Generation of ${}^{4}{}_{2}\mathrm{He}$ in surface layers in Pd cathode were interpreted by reactions $n + {}^{6}{}_{3}\mathrm{Li} \rightarrow {}^{7}{}_{3}\mathrm{Li}^{*} \rightarrow {}^{4}{}_{2}\mathrm{He}$ (2.1 MeV) + ${}^{3}{}_{1}\mathrm{H}$ (2.7 MeV)

A5-2-2. Reduction of decay constant of the unstable nucleus 3919K *.

R. Bush [54] observed the excess heat generation and nuclear transmutations ${}^{23}{}_{11}\mathrm{Na} \rightarrow {}^{24}{}_{12}\mathrm{Mg}$ and ${}^{39}{}_{19}\mathrm{K} \rightarrow {}^{40}{}_{20}\mathrm{Ca}$ in electrolytic systems;

$$\mathrm{Ni(alloy)/H_2O{+}K_2CO_3/K \text{ and } Ni(alloy)/H_2O{+}Na_2CO_3/Na.}$$

In a case of ${}^{40}{}_{20}\mathrm{Ca}$ production (from ${}^{39}{}_{19}\mathrm{K}$) with a Ni cathode,the average excess heat was $Q = 0.58 \pm 0.15$ J/s and the generated calcium atom was 4.8 x 10^{18}/15 d. In the case of ${}^{24}{}_{12}\mathrm{Mg}$ production (from ${}^{23}{}_{11}\mathrm{Na}$) with a Ni alloy cathode,only the relative excess heat to the former case was given as $Q_{Na}/Q_{K} = 1.90 \pm 0.33$.

It should be notice that the decay time of ${}^{39}{}_{19}\mathrm{K}$ into ${}^{40}{}_{20}\mathrm{Ca}$ by beta decay is known as $\sim 10^{9}$ y in nuclear physics. This data set were analyzed on the TNCF model in [4 (Sec. 11.11a)] assuming the decay time shortening of ${}^{39}{}_{19}\mathrm{K}$ in the surface layer.

Table 4.

Isotope	Natural abundance (%)
$^{234}{}_{92}$U	5.5×10^{-3}
$^{235}{}_{92}$U	0.72
$^{238}{}_{92}$U	99.28

A5-2-3. Reduction of Decay Constant of Radioactive Uranium

Dash et al. measured the change of radioactivity of uranium in contact with hydrogen [50], [51]. In the first experiment [50], the sample of uranium was codeposited with hydrogen on the substrate from a light water electrolyte and in the second experiment [51] the sample of uranium foils was attached to the cathode of a glow discharge apparatus to be bombarded by hydrogen or deuterium ions. The rates of alpha, beta, and gamma radiation emissions per unit mass of uranium were significantly greater in the experimental samples in both experiments compared with the original uranium.

It is known that uranium becomes a crystal belonging to monoclinic space group $C_{2h}{}^3$ with 2 atoms in each crystallographic cell (called α-phase) at room temperature (α-phase stable under 668 °C). The dimensions of the cell are: *a*=2.829A, *b*=4.887A, *c*=3.308A (axial ratios $a : b : c = 0.5791 : 1 : 0.6771$). It is known that there formed uranium hydride α-UH_3 when α-uranium is in contact with hydrogen [55]. The formation of uranium hydride is recognized as a hazard during the storage of uranium metal owing to its potentially pyrophoric properties.

In connection with the experiments by Dash et al. [50], [51], we notice the structure of α-UH_3 and the energy levels of outer most neutrons in uranium nuclei with natural abundances of isotopes are shown in Table A5-1;

There is an interesting structure of the uranium nuclei and the protons in the uranium hydride α-UH_3 explained as follows;

“The crystal lattice consists of a uranium atom surrounded by 6 uranium atoms and 12 hydrogen atoms, with the hydrogen atoms occupying large tetrahedral spaces in the lattice.” [56]

“In the crystal, U-H-U bonds exist through hydrogen.” [57]

This feature reminds us the carbon-hydrogen structure in XLPE (cf. Sec. 2.3.3) and suggests a possible realization of the super-nuclear interaction of neutrons in lattice nuclei $^{A}_{92}$U mediated by occluded protons/deuterons.

Another data advantageous for the formation of the neutron bands is the neutron energy levels of lattice nuclei at around zero discussed in Sec. 3.2.1. Unfortunately, the data shown in Fig. 3 (in Sec. 3.2.1) is only for *A* = 18–210 not covering the necessary data for $^{A}_{92}$U (*A* = 234, 235, 238). So, we have to use our wishful thinking that the tendency of the neutron levels near zero energy at around *A* = 200 seen in Fig. 3 may extends to higher values of *A* up to 240.

Then, we may expect that the interaction of the neutron Bloch waves and the lattice nuclei $^{A}_{92}$U results hopefully in reduction of decay constants in accordance with the experimental data obtained by Dash et al. [50], [51].

A5-3. Forced Nuclear Fission Induced by Interaction with Neutron Bloch Wave in the CFP

There are many experimental data sets in the CFP showing appearance of new elements or new nuclei not found before the experiments [4 (Sec. 9), 5 (Sec. 2.5), 6 (Appendix C), 49 (Sec. 6.4.4)]. It should be noticed that it is necessary to assume a mechanism where involved a neutron drop $^{A}{}_{Z}\Delta$, an aggregate composed of (*A*–*Z*) neutrons and *Z* protons in the neutron bands, for the explanation of the experimental facts showing appearance of nuclei with large shifts of the mass number *A* and the proton number Z from those of preexisted nuclei in the system [5 (Sec. 2.4.2)]. Assuming the existence of the neutron drop, we could explain the curious data showing appearance of new nuclei with large shifts of *A* and *Z* from original species preexisted in the system [5 (Sec. 2.5.3), [40 (Secs. 5.2 and 6.2)].

Table 5. Concentrations of impurities (Atomic weight percent) found in virgin Pd after three weeks of electrolysis (EDS). (Table 2 of [58] simplified omitting data not related with the experiment reported in the paper.)

Element	Amount at 1μm depth after 3 weeks Electrolysis (at %)
Mg	6.7 ± 1.0
Ag	1.9 ± 1.0
Si	10.2 ± 1.0
Cl	3.0 ± 1.0
K	1.1 ± 1.0
Ca	19.9 ± 1.0
Ti	1.6 ± 1.0
Fe	10.5 ± 1.0
Cu	1.9 ± 1.0
Zn	4.2 ± 1.0
Pt	7.1 ± 1.0
Pd	31.9 ± 1.0

We cite in this Section A5-3 only three papers as typical examples of investigation in this field leaving explanations of last two papers in our original works [5 (Sec. 2.5.3), 5 (Appendix C6)].

A5-3-1. J. O'M. Bockris and Z. Minevsky, "Two Zones of 'Impurity' observed after Prolonged Electrolysis of Deuterium on Palladium," Infinite Energy Nos. 5 & 6, pp. 67–73 (1995–6), ISSN 1081-6372. [58]

The experimental data obtained by Bockris and Minevsky as shown in the sentences cited below from their paper [58] is only explicable by nuclear fission reactions of nuclei generated by absorptions of thermal neutrons in neutron bands formed by the super-nuclear interaction between lattice nuclei.

"Energy dispersive spectroscopy was also used to seek material which might be further into the metal. In EDS, the maximum intensity of the signal arises from a greater depth than that of XPS (L). In fact, for palladium, for a 20 kV X-ray beam, the escape depth maximizes at about 2 μm inside the palladium and the signals found both after one hour's electrolysis, and then after three week's electrolysis, are shown in Figures 2 and 3, respectively (Figs. 2 and 3 are not shown in this citation). It is seen that new nuclei have appeared at this depth in the presence of hydrogen at high fugacity (overpotential more than 0.5 volts).

The concentration of the new atoms is in the range 1-10 atomic percent. The materials shown in Table 2 (cited as Table A2-2 below) have no relationship to the impurities in the solution (further, diffusion of the materials cited in Figures 2 and 3, into depth of $\sim 1\mu$ could not occur in three weeks)" [58].

Similar experimental data sets are obtained by many researchers and we cite two typical data below from them leaving their explanations in our works [5 (Sec. 2.5.3), (Appendix C6)].

A5-3-2. G.H. Miley, G. Name, M.J. Williams, J.A. Patterson*, J. Nix*, D. Cravens*, and H. Hora, "Quantitative Observation of Transmutation Products occurring in Thin-Film Coated Microspheres during Electrolysis," *Proc. ICCF-6,* pp. 629–644 (1996), NEDO, The Institute of Applied Energy, 1996 [59].

A5-3-3. G.H. Miley and J.A. Patterson, "Nuclear Transmutations in Thin-Film Nickel Coatings undergoing Electrolysis," *J. New Energy* No. **1-3**, pp. 5–30 (1996), ISSN 1086-8259 [60].

A5-4. Attempt to Formulate the Effect of the Neutron Bloch Wave on the Nuclear Process in the Lattice Nuclei

In the Subsections A5-1 to A5-3 in the Appendix A5, we have shown wonderful experimental facts of the stabilization of unstable nuclei in the CFP. It is then necessary to give a possible explanation for the experimental facts. One of

the possible explanations for the change of nuclear processes in the lattice nuclei in the CF materials is the effect of the trapped neutron to the stabilization of unstable nuclei incomprehensible at present from our knowledge of the neutron-nucleus interaction.

In the phenomenological approach to the CFP, we have mainly used single-particle interaction and many-body interaction sometimes interchangeably as we want to explain some events such as the nuclear transmutations by fission only. This may be a source of distrust of our approach from people who want to have a solid basis to treat physics of nuclear interactions. Actually, the physics of the CFP revealed by the phenomenological approach is fundamentally a many-body problem composed of nucleons in lattice nuclei and occluded protons/deuterons. Then, it may be necessary to treat the problem taken up in this Appendix A5 as a many-body problem.

To see the possibility of understanding a most simple decay process considered in Appendix A5-1, we tried to formulate a mechanism with participation of a single neutron in interaction with an unstable nucleus $^{10}{}_{5}$B. Even in this example, the calculation needed to obtain the final result is unmanageable and we have to look forward to future research to realize the drawn framework.

Possible Reactions of a Thermal Neutron n and 105B – An Example of the Process as a Single Particle Problem [47], [48]

In the nuclear reactions observed by T.O. Passell, we can assume the reaction between one of trapped neutrons in the neutron bands and a $^{10}{}_{5}$B or $^{11}{}_{5}$B nucleus occurs at an irregular site of the cathode.

The natural abundances and the absorption cross-sections of a thermal neutron of these isotopes are as follows:

Nucleus	Natural abundance	σ_n ($\times 10^{24}$ cm^2) for thermal neutron (n_ε= 1/40 eV)
$^{10}{}_{5}$B	19.78	3.837×10^{3}
$^{11}{}_{5}$B	80.22	5.075×10^{-3}

(1 barn = 10^{-28} m^2 (100 fm^2) = 10^{-24} cm^2)

The main nuclear reactions between impurity boron nucleus $^{10}{}_{5}$B in the Pd cathode used in an electrolytic CF experiment of the system Pt/D_2O/Pd that successfully produced excess heat [47], [48] are shown in the following Eq. (A5-1) in vacuum:

$$n + {}^{10}{}_{5}\mathrm{B} \rightarrow {}^{11}{}_{5}\mathrm{B}^{*} \rightarrow {}^{11}{}_{5}\mathrm{B} + \gamma. \tag{A5-1}$$

The excited nucleus $^{11}{}_{5}$B* interacts with neutron Bloch waves $n(kT)$'s in neutron bands giving the excitation energy to the phonons φ's through interaction with them (in our TNCF model):

$$n(kT)\text{'s} + {}^{11}{}_{5}\mathrm{B}^{*} \rightarrow {}^{11}{}_{5}\mathrm{B} + n'(3kT/2 + \varepsilon_\gamma)\text{'s} \rightarrow {}^{11}{}_{5}\mathrm{B} + \varphi\text{'s}, \tag{A5-2}$$

where ε_γ is the excess energy of $^{11}{}_{5}$B* compared to $^{11}{}_{5}$B, *φ's* represent phonons in the cathode excited by the interaction of the epithermal and higher energy neutrons $n'(3kT/2 + \varepsilon_\gamma)$'s and the lattice.

The decay times τ_1 and τ_2 of the competitive stabilization processes (A5-1) and (A5-2) are qualitatively estimated as follows.

(1) The decay time τ_1 of the gamma emission of the excited state of B-11 ($^{11}{}_{5}$B*) may be found somewhere in data books.

$$\tau_1 \sim \mathrm{xxx}.$$

(2) Interaction of $^{11}{}_5\mathrm{B}^*$ and a thermal neutrons $n(kT)$ in neutron bands results in the stable nucleus $^{11}{}_5\mathrm{B}$ and an energetic neutrons n' (kT + ε_γ) with a decay time $\boldsymbol{\tau}_2$ (which could be calculated by quantum mechanics of nucleus):

$$n(kT) + {}^{11}{}_5\mathrm{B}^* \rightarrow {}^{11}{}_5\mathrm{B} + n' \,(\mathrm{kT} + \varepsilon_\gamma). \tag{A5-3}$$

Assuming existence of trapped neutrons with a density $n_n \sim 10^{10}$ cm^{-3} in neutron bands, we can estimate the order of magnitude of dissipation probability per second by this mechanism adding up individual process (A5-3) to obtain the decay time $\boldsymbol{\tau}_3$ (assuming the process is additive):

$$\boldsymbol{\tau}_3 \sim \mathrm{yyy}.$$

We expect a following result for the relation between $\boldsymbol{\tau}_1$ and $\boldsymbol{\tau}_3$:

$$\boldsymbol{\tau}_1 \sim \mathrm{xxx} \gg \boldsymbol{\tau}_3 \sim \mathrm{yyy}.$$

Unfortunately, the calculation of $\boldsymbol{\tau}_2$ is not easy for us, and furthermore there is no guarantee the time constant $\boldsymbol{\tau}_3$ is calculated by simply adding the process (A5-3).

Anyway, we leave this calculation for our future plans.

Acknowledgement

The author would like to express his heartfelt gratitude to Dr. Kaori Kaki and Dr. Masayuki Ohta for their kind communications on the problem discussed in Appendix A5 in this paper.

References

[1] M. Fleischmann, S. Pons and M. Hawkins, *J. Electroanal. Chem*. **261**, 301 - 308 (1989), ISSN: 1572-6657.

[2] S.E. Jones, E.P. Palmer, J.B. Czirr, D.L. Decker, G.L. Jensen, J.M. Thorne and S.E. Tayler, *Nature* **338**, 737–740 (1989), ISSN 0028-0836.

[3] H. Kozima, "Trapped Neutron Catalyzed Fusion of Deuterons and Protons in Inhomogeneous Solids," *Transactions of Fusion Technol.*, **26** (4T-2, Fuste8(4) 1-540 (1994), pp. 580–515, ISSN 0748-1896.

[4] H. Kozima, *Discovery of the Cold Fusion Phenomenon – Development of Solid State-Nuclear Physics and the Energy Crisis in the* 21^{st} *Century* –, Ohtake Shuppan Inc., 1998, ISBN 4-87186-044-2. The "References" in this book are posted at the CFRL (Cold Fusion Research Laboratory) Website; http://www.kozima-cfrl.com/Books/bookse/bookse.html

[5] H. Kozima, *The Science of the Cold Fusion Phenomenon*, *– In Search of the Physics and Chemistry behind Complex Experimental Data Sets –*, 1^{st} Edition, Elsevier, Amsterdam, 2006, ISBN-13: 978-0-08045-110-7.

[6] H. Kozima, "Development of the Solid State-Nuclear Physics," *Proceedings of JCF19,* **19-15**, pp. 112–147 (2019), ISSN 2187-2260.

[7] E. Storms, *The Science of Low Energy Nuclear Reactions*, World Scientific Publishing, 2007, ISBN-10 981-270-620-8.

[8] H. Kozima, "The Cold Fusion Phenomenon in the Gas-Solid System – A Review –," *J. Condensed Matter Nuclear Science,* **40**, (2025), ISSN 2227-3123. (to be published)

[9] H. Kozima, "Quantum Physics of Cold Fusion Phenomenon," in F. Columbus and V. Krasnoholovets Eds., *Developments in Quantum Physics*, pp. 167–196, Nova Science Publishers, Inc., New York, 2004, ISBN 1-59454-003-9.

[10] H. Kozima, "Physics of the Cold Fusion Phenomenon," *Proc. ICCF13* (June 25 – July 1, 2007, Dagomys, Sochi, Russia), pp. 690–703 (2008), ISBN 978-5-93271-428-7.

[11] H. Kozima, "Cold Fusion Phenomenon in Open, Nonequilibrium, Multi-component Systems – Self-organization of Optimum Structure," *Proc. JCF13,* **13-19**, pp. 134–157 (2013), ISSN 2187-2260.

[12] H. Kozima, "The Cold Fusion Phenomenon – Nuclear Transmutations in the CF Materials at Around Room Temperature –," *International Journal of High Energy Physics* **8 (1),** pp. 1–12 (2021), ISSN 2376-7448.

[13] H. Kozima, "Peculiarities of Physics and Chemistry in the Transition Metal Hydrides," *J. Condensed Matter Nucl. Sci.* **37**, pp. 98–110 (2023), ISSN 2227-3123.
[14] J.M. Blatt and V.F. Weisskopf, *Theoretical Nuclear Physics*, John Wiley & Sons, New York, 1952, ISBN 10: 0-471-08019-5.
[15] H. Kozima, "On the 30^{th} anniversary of Discovery of the Cold Fusion Phenomenon," *Infinite Energy* No. **145**, pp. 28–34 (2019), ISSN 1081-6372.
[16] H. Kozima and K. Kaki, "H. Kozima and K. Kaki, "Atomic Nucleus and Neutron — Nuclear Physics Revisited with the Viewpoint of the Cold Fusion Phenomenon," *Proc. JCF14:***14-5**, pp. 47 - 76 (2014). ISSN 2187-2260.
[17] M.C.H. McKubre, S. Crouch-Baker, A.M. Riley, S.I. Smedley and F.L. Tanzella, "Excess Power Observed in Electrochemical Studies of the D/Pd System," *Proc. ICCF3* (Oct. 21–25, 1992, Nagoya, Japan), pp. 5 - 19, Universal Academy Press, Inc., Tokyo, 1993, ISBN: 4-946443-12-6.
[18] M.C.H. McKubre, S. Crouch-Baker, R.C. Rocha-Filho, S.I. Smedley, F.L. Tanzella, T.O. Passell and J. Santucci, "Isothermal Flow Calorimetric Investigations of the D/Pd and H/Pd Systems," *J. Electroanal. Chem.*, **368**, 55–66 (1994), ISSN: 1572-6657.
[19] M. C. H. McKubre, S. Crouch-Baker, F. L. Tanzella, S. I. Smedley, M. Williams, S. Wing, M. Maly-Schreiber, R. C. Rocha-Filho, P. C. Searson, J. G. Pronko and D. A. Kohler, *Development of Advanced Concepts for Nuclear Processes in Deuterated Metals, TR-104195*, 1994, Electric Power Research Institute. This book is available at following site: http://my.epri.com/portal/server.pt?Abstract_id=TR-104195
[20] H. Kozima, "From the History of CF Research," *Proc. JCF16,* **16-13,** pp. 116–157 (2016), ISSN 2187-2260.
[21] R.L. Mills and S.P. Kneizys, "Excess Heat Production by the Electrolysis of an Aqueous Potassium Carbonate Electrolyte and the Implications for Cold Fusion," *Fusion Technol.*, **20**, 65–81 (1991), ISSN: 0748-1896.
[22] R.T. Bush, "A Light Water Excess Heat Reaction suggests that 'Cold Fusion' may be 'Alkali-Hydrogen Fusion'," *Fusion Technol.* **22**. 301–322 (1992). ISSN 0748-1896
[23] R.T. Bush and D.R. Eagleton, "Experiment Supporting the Transmission Resonance Model for Cold Fusion in Light Water: I. Correlation of Isotopic and Elemental Evidence with Excess Heat," *Proc. ICCF3*, pp. 405–408 (1993). ISBN 4-946443-12-6
[24] R.T. Bush and D.R. Eagleton, "Evidence for Electrolytically Induced Transmutation and Radioactivity Correlated with Excess Heat in Electrolytic Cells with Light Water Rubidium Salt Electrolytes," *Trans. Fusion Technol*. **26**, 344–354 (1994). ISSN 0748-1896.
[25] T. Hanawa, "X-ray Spectrometric Analysis of Carbon Arc Products in Water," *Proc. ICCF8*, pp. 147–152 (2000), ISBN 88-7794-256-8.
[26] H. Kozima and M. Tada, "The Cold Fusion Phenomenon in Hydrogen-graphites," *Proc. JCF12* (Kobe, Japan, December 17–18, 2011), pp. 77–92 (2012), ISSN 2187-2260.
[27] H. Kozima, "From the History of CF Research – A Review of the Typical Papers on the Cold Fusion Phenomenon –," *Proc. JCF16,* **16-13,** pp. 116–157 (2016), ISSN 2187-2260.
[28] T. Kumazawa, W. Nakagawa and H. Tsurumaru, "A Study on Behavior of Inorganic Impurities in Water Tree" *Electrical Engineering in Japan* **153**, 1–13 (2005).
[29] T. Kumazawa, W. Nakagawa and H. Tsurumaru, "Experimental Study on Behavior of Bow-tie Tree Generation by Using Heavy Water" (in Japanese) *IEEJ Trans. FM,* **126**, 863–868 (2006). (Experiment with Heavy Water)
[30] T. Kumazawa, R. Taniguchi, "A Study on Detection of Weak X/γ-ray with growth of Water Trees," *IEEJ Transactions on Fundamental and Materials,* **132**, 1045–1052 (2012) (in Japanese).
[31] H. Kozima, "Nuclear Transmutations in Polyethylene (XLPE) Films and Water Tree Generation in Them (2)," *Proc. JCF16,* **16-17**, pp. 210 - 215 (2016), ISSN 2187-2260.
[32] V.I. Vysotskii, A.A. Kornilova and I.I. Samoylenko, "Experimental Discovery of the Phenomenon of Low-Energy Nuclear Transmutation of Isotopes (^{55}Mn $\rightarrow$ ^{57}Fe) in Growing Biological Cultures," *Proc. ICCF6*, pp. 687–693 (1996).
[33] V.I. Vysotskii and A.A. Kornilova, *Nuclear Transmutation of Stable and Radioactive Isotopes in Growing Biological Systems*, Pentagon Press, India, 2009.
[34] V.I. Vysotskii and A.A. Kornilova," Nuclear Transmutation of Isotopes in Biological Systems (History, Models, Experiments, Perspectives), *Journal of Scientific Exploration*, **23**, pp. 496–500 (2009)
[35] V.I. Vysotskii and A.A. Kornilova," Microbial Transmutation of Cs-137 and LENR in growing biological systems," *Current Science,* **108**, pp. 142–146 (2015).

[36] H. Kozima, "Biotransmutation as a Cold Fusion Phenomenon," *Proc. JCF16,* **16-18,** pp. 216 - 239 (2016), ISSN 2187-2260.
[37] H. Kozima, "Non-localized Proton/Deuteron Wavefunctions and Neutron Bands in Transition-metal Hydrides/Deuterides," *Proc. JCF9* (March 28–29, 2009, Shizuoka, Japan), pp. 84–93 (2009), ISSN 2187-2260.
[38] C.M. Mate and G.A. Somorjai, "Delocalized quantum nature of hydrogen adsorbed on the Rh (111) crystal surface" *Phys. Rev*. **B34**, 7417–7420 (1986).
[39] K.R. Christmann, "Hydrogen Sorption on Pure Metal Surface" in Z. Paal and P.G. Menon Eds. *Hydrogen Effects in Catalysis*, Marcel Dekker Inc., N.Y., 1988. ISBN 0-8247-7774-3.
[40] H. Kozima, "The Cold Fusion Phenomenon – What is It?" *Proc. JCF14:* 14-16, pp. 203–230 (2014). ISSN 2187-2260.
[41] A. Bohr and B.R. Mottelson, *Nuclear Structure* I, Benjamin, New York, 1969.
[42] I. Wiedenhover, "Exotic Nuclei," *Lecture note given at National Nuclear Physics Summer School*, 7/16/2007 Tallahassee, Florida.
[43] K. Riisager, "Neutron Halo States" *Rev. Mod. Phys*. **68**, 1106–1116 (1994).
[44] P.G. Hansen, "Nuclear Halo: Structure and Reactions" *Nuclear Physics*, **A588**, 1c–10c (1995)."
[45] Y. Yoshinaga, *What is a complex system?* Kodansha, Tokyo, 1996, ISBN 4-06-149328-0 C0242. (in Japanese)
[46] J.W. Negele and D. Vautherin, "Neutron Star Matter at Sub-nuclear Densities," Nuclear Phys., A207, pp. 298–320 (1973), ISSN 1873-1554.
[47] T.O. Passell, "Search for Nuclear Reaction Products in Heat Producing Palladium," *Proc. ICCF6*, pp. 282–290 (1996).
[48] T.O. Passell, "Search for Nuclear Reaction Products in Heat Producing Palladium," *Proc. ICCF7,* pp. 309–313 (1998).
[49] H. Kozima, "Nuclear Transmutations (NTs) in Cold Fusion Phenomenon (CFP) and Nuclear Physics," *Proc. JCF14:***14-15,** pp. 168 - 202 (2014). ISSN 2187-2260.
[50] G. Goddard and J. Dash, "Characterization of Uranium Codeposition with Hydrogen on Nickel Cathodes," *Trans. American Nuclear Soc.*, **83**, 376 (2000). ISSN 0003-018X.
[51] J. Dash, I. Savvatimova, S. Frantz, E. Weis and H. Kozima, "Effects of Glow Discharge with Hydrogen Isotope Plasmas on Radioactivity of Uranium" *Proc. ICCF9*, pp. 77–81 (2003), ISSN 7-302-06489-X/O·292.
[52] J.R. Morrey, M.R. Caffee, H. Farrar, IV, N.J. Hoffman, G.B. Hudson, R.H. Jones, M.D. Kurz, J. Lupton, B.M. Oliver, B.V. Ruiz, J.F. Wacker and A. Van, "Measurements of Helium in Electrolyzed Palladium," *Fusion Technol*., **18**, 659–668 (1990), ISSN 0748-1896.
[53] H. Kozima,S. Watanabe,K. Hiroe,M. Nomura,M. Ohta and K. Kaki, "Analysis of Cold Fusion Experiments generating Excess Heat,Tritium and Helium," *J. Electroanal. Chemistry* **425**, pp. 173–178 (1997), ISSN 1572-6657.
[54] R.T. Bush, "A Light Water Excess Heat Reaction suggest that 'Cold Fusion' may be 'Alkali-Hydrogen Fusion"' *Fusion Technol.* **22**, 301(1992), ISSN 0748-1896.
[55] H. Godfrey, C. Broan, D. Goddard, G. Woodhouse, P. Durham, A. Diggle and J. Bradshaw, "Formation and Physical Properties of Uranium Hydride under Conditions relevant to Metallic Fuel and Nuclear Waste Storage," *J. Nuclear Materials*, **477**, pp. 236–245 (2016), ISSN 1873-4820.
[56] Amit Arora (2005). *Text Book Of Inorganic Chemistry*. Discovery Publishing House. p. 789. ISBN 81-8356-013-X
[57] G. Singh (2007). *Environmental Pollution*. Discovery Publishing House. ISBN 81-8356-241-8
[58] J.O'M. Bockris and Z. Minevsky, "Two Zones of 'Impurity' observed after Prolonged Electrolysis of Deuterium on Palladium," *Infinite Energy* Nos. **5 & 6**, pp. 67–73 (1995–6), ISSN 1081-6372.
[59] G.H. Miley, G. Name, M.J. Williams, J.A. Patterson, J. Nix*, D. Cravens, and H. Hora, "Quantitative Observation of Transmutation Products occurring in Thin-Film Coated Microspheres during Electrolysis,*" Proc. ICCF-6,* pp.629–644 (1996), NEDO, The Institute of Applied Energy, 1996.
[60] G.H. Miley and J.A. Patterson, "Nuclear Transmutations in Thin-Film Nickel Coatings undergoing Electrolysis," *J. New Energy* No. **1-3**, pp. 5–30 (1996), ISSN 1086-8259.